Journal of Marine Systems, 1 (1991) 217–228
Elsevier Science Publishers B.V., Amsterdam

Predictability and variability of a coupled ocean–atmosphere model

B.N. Goswami [1] and J. Shukla

Center for Ocean-Land-Atmosphere Interactions, Department of Meteorology, University of Maryland, College Park, MD 20742, U.S.A.

Received December 7, 1989; revised version accepted December 20, 1989

ABSTRACT

Goswami, B.N. and Shukla, J., 1991. Predictability and variability of a coupled ocean–atmosphere model. J. Mar. Syst., 1: 217–228

This paper presents a summary of our research on the predictability and variability of a coupled ocean–atmosphere model (Cane et al., 1986; Zebiak and Cane, 1987). The detailed description of our work including the modeling experiments and the results are being presented elsewhere in the form of two scientific papers. In the first paper (Goswami and Shukla, 1990a) we have investigated the predictability of a coupled ocean–atmosphere model and in the second paper (Goswami and Shukla, 1990b) we have proposed a mechanism for aperiodic variability in a coupled ocean–atmosphere model.

We first integrated the model for 24 years with prescribed wind stress forcing from observations beginning with January, 1964. We refer to this as the control run. We then used the initial conditions from this simulations to integrate the coupled ocean–atmosphere model. We integrated the coupled model for a period of 36 months for 181 separate initial conditions corresponding to the period January 1970 through January 1985 of the control run. We have compared the forecasts of *SST* by the coupled model with the observed and the control simulation. We have noted some systematic errors in the model suggesting that forecasts can be further improved by removing the systematic errors. We find that the *SST* forecasts with the coupled model are better than persistence for the first three months. It is also worth noting that the root mean square error between the control run initial conditions and observations are comparable to the standard deviations of the observations themselves.

We have also integrated the coupled model for 15 years by slightly perturbing the surface winds initially. Using a large ensemble of such identical twin experiments we have found that the growth of small initial errors in this coupled model is characterized by two well separated time scales. The fast time scale gives an error doubling time of 5 months and the slow scale gives an error doubling time of about 15 months. We are encouraged by the prospects of extended range predictions using coupled models because of the existence of the slow time scale, however, in order to realize the potential predictability of the coupled, model it would be essential to control the fast time scale error growth.

We have also investigated the possible mechanisms responsible for the aperiodic behavior of this model. Sensitivity of the coupled model's variability to the nonlinearily associated with the coupling processes is studied. The atmospheric heating associated with the anomalous low level convergence (convergence feedback) seems to play an important role in producing the model's aperiodic variability. We show that this feedback has a strong seasonality due to its dependence on the seasonal mean convergence. In the absence of the convergence feedback, the standard parameters of the Cane and Zebiak model give a periodic variability with a periodicity of about 4 years. This feedback produces a broadening of the basic low frequency spectrum through the introduction of a high frequency component.

[1] Permanent affiliation: Centre for Atmospheric Sciences, Indian Institute of Science, Bangalore – 560012, India

0924-7963/91/$03.50

Introduction

We have investigated the predictability and variability of a coupled ocean–atmosphere model by examining the growth of small initial errors during the evolution of the coupled system. The details of this study are being published elsewhere (Goswami and Shukla, 1990a, b). The salient features of our study are summarized in this article.

We have used the model by Cane et al. (1986) and Zebiak and Cane (1987, hereafter referred as ZC). The standard set of parameters given in ZC is used. This version of the model including the climatologies required was provided to us by the authors. The reader is referred to the above references for the details about the model and the parameters used. Further insight into the dynamics and thermodynamics of such a model is provided by Battisti (1988).

The control experiment

In order to carry out prediction and predictability studies with the coupled model, a data set representing the true interannual variations of both the atmosphere and ocean is required. Ocean circulation data over a long period of time is not available. Surface wind analyses over the Pacific are, however, available over a relatively long period of time (Goldenberg and O'Brien, 1981; Barnett, 1983). Therefore, we chose to define the interannual variations of the tropical ocean as given by forcing the ocean model with the observed wind stress anomalies. These observed wind stress anomalies are based on subjective analysis of surface winds obtained from ship reports by Goldenberg and O'Brien (1981). A 1-2-1 filter in time, longitude and latitude was applied to the analyzed winds. In order to remove an unrealistic trend, the anomalies used are deviations from average of the same calendar month over the previous four years (Cane et al., 1986; Cane and Zebiak, 1987). These analyses were also provided to us by Cane and Zebiak. It consists of monthly mean values for the period January, 1964 to May, 1988. The resolution is $2° \times 2°$ and the analyzed data extend from 29°S to 29°N and 126°E to 70°W. Our control experiment corresponds to this forced run in which the ocean model is forced by these observed wind stress anomalies. Starting with January 1970, the ocean fields as well as the atmospheric fields produced by the atmospheric model during this run (although they were not used to force the ocean model) are saved once every month. These fields provide us the necessary initial conditions for the prediction experiments to be described later.

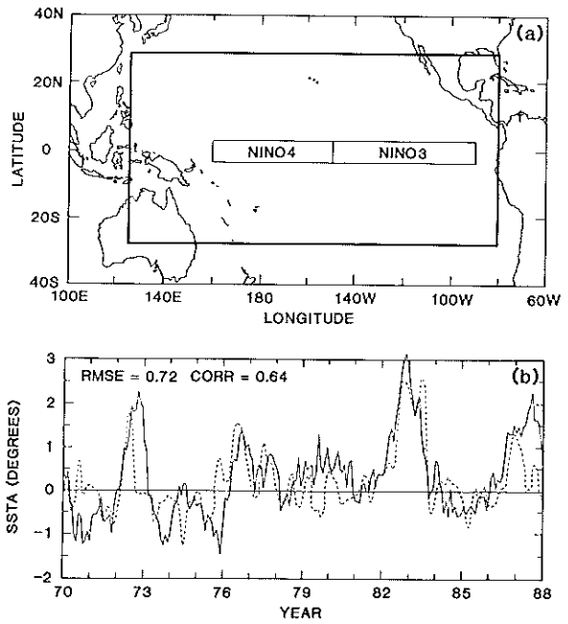

Fig. 1. (a) The geographical domain for the ocean model and the two regions NINO3 and NINO 4. (b) NINO3 (5°N to 5°S and 150°E to 90°W) averaged SSTA in the control experiment (dashed curve) versus the observed (solid curve) over the same region. The RMS error and correlation between the two series are shown.

The physical domain for the ocean model and locations of the regions NINO3 and NINO4 are shown in Fig. 1a. the performance of the ocean model in simulating the interannual variations is shown in Fig. 1b, where the NINO3 (5°S to 5°N and 150°W to 90°W) averaged *SST* anomalies (SSTA) simulated by the forced model is compared with observations from the Climate Analysis Center (CAC). It is seen that the model simulates the warm events reasonably well. However, the correlation between the observed and simulated SSTA is poor during the intermediate periods. The rms error between the observed and

simulated *SST* is 0.72° C. This is comparable to the standard deviation (= 0.71° C) of the simulated time series but is smaller than the standard deviation (= 0.92° C) of the observed sea surface temperature anomaly over NINO3 region (NINO3 SSTA). This discrepancy between the model simulation and the observation may be partly due to the inadequacy of the ocean model and partly due to the errors in the analysis of wind stress used as observations.

The prediction experiments

We have carried out a large ensemble of prediction experiments. Each experiment is started with an initial condition saved once every month during the control experiment, starting with January 1970. The coupled model then determines the future evolution for a duration of 36 months. This means that the initial conditions for the ocean are model simulations forced by the observed wind stresses, but during the prediction period, the coupled model evolves as an interacting coupled system. In this manner, 181 forecast experiments were carried out for 181 initial conditions corresponding to each month during the period January 1970 through January 1985.

To illustrate the nature of evolution of these prediction, NINO3 SSTA from the coupled model are shown in Fig. 2. It shows a rich variety of dependence of the predictions on the initial conditions. The model is successful in capturing the major El Niño events, however, for many cases a large warm event is predicted even when there is no warm event in the control.

The prediction minus control errors averaged over all the 181 predictions and the persistence errors averaged for all the 181 initial conditions are shown in Fig. 3. It also shows the standard deviation of the control NINO3 SSTA. It should be noted that the predictions are better than the persistence only for the first three months. Also, the errors become larger than the natural variability (i.e., the standard deviation) after three months. The errors tend to saturate by about 9 months.

We noted that the model predictions show a systematic error. We shall define the systematic error as the average prediction error (mean of all the predictions minus means of all the verifications from the control run). This systematic error of the model is shown in Fig. 4a by the solid curve. Largest positive bias occurs for a lag of about 12 months. We examined whether the prediction skill could be improved by removing this systematic error from the predictions. The errors calculated after subtracting the systematic error from the predictions is shown in Fig. 4b by the dotted curve. It is seen that the skill of the predictions beyond three months improves to some extent by this procedure. However, the errors remain larger than persistence beyond three months. The possibility of improving the skill using lagged averaged forecast method is explored in Fig. 4b. It shows that if we remove the systematic error and average the six predictions initiated from the last six months, the predictions show significant improvement beyond six months, however, the error is still higher than long term standard deviation of the control.

The predictability experiments

Having derived some measure of the current predictive skill of the coupled model used in this study, we addressed the more fundamental question on the theoretical limit on the predictability of such coupled systems. We have done this by adopting methods used in the classical predictability studies of the atmosphere to determine the time scale of growth of small initial errors. We shall use the control run to define the initial conditions for coupled model runs. Following Lorenz (1982) we calculate the growth of error between two coupled model runs for which initial conditions were only one month apart in the control run. We repeated these calculations for initial conditions being 2, 3, 4,... 12 months apart in the control run. Since all the predictions made so far were only for a duration of three years, it was found that small initial errors (such as the one month forecast errors) did not saturate during the course of three years integrations.

In order to obtain a more reliable estimate of the growth rate, we decided to carry out a series of identical twin experiments of sufficiently long during. First, we conducted 151 control forecast ex-

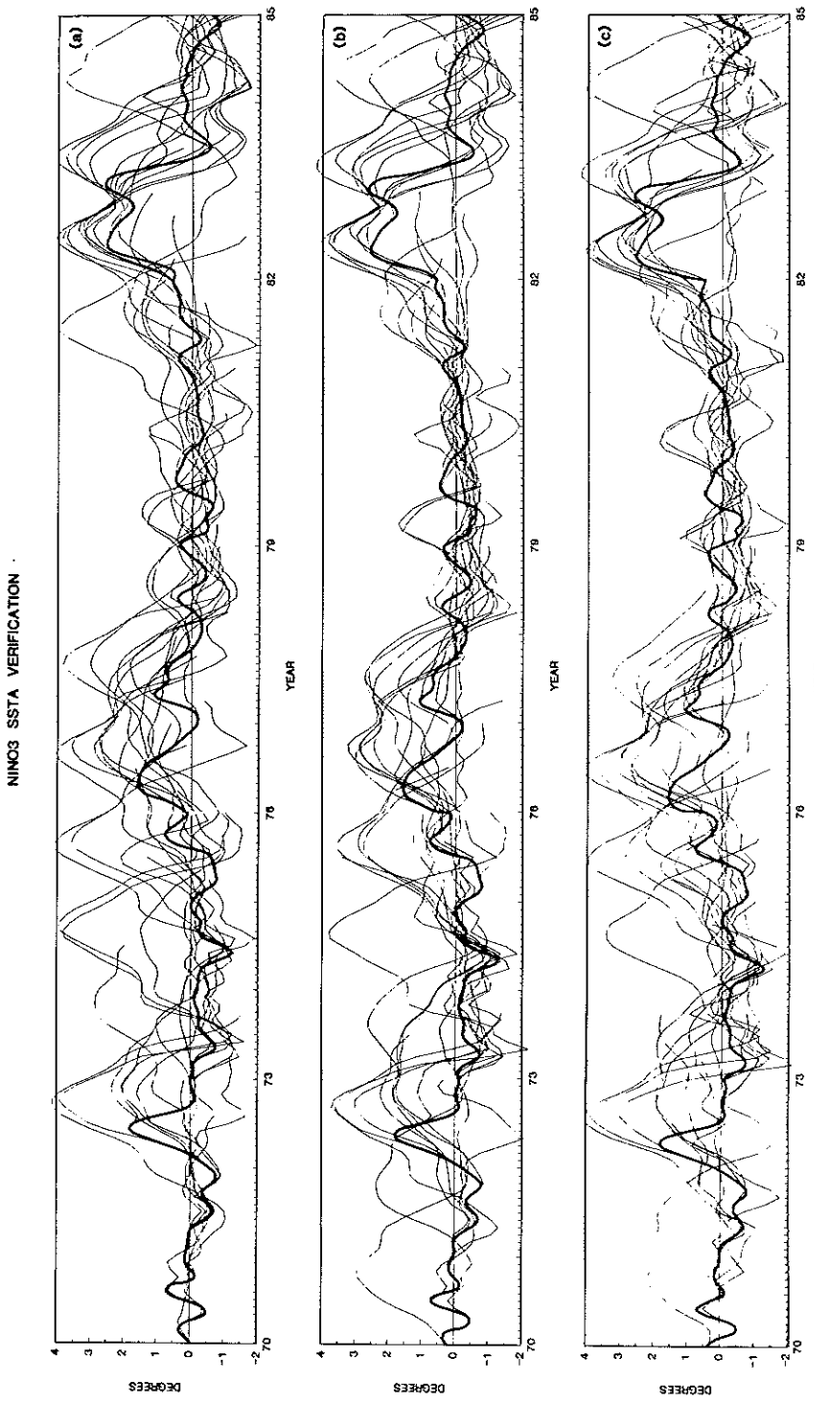

Fig. 2. The complete ensemble of predictions for NINO3 SSTA are shown. The heavy curve represents the control while the light curves are the predictions. Every third predictions are shown in each panel for clarity. (a) predictions starting from January 1970, (b) predictions starting from February 1970 and (c) predictions starting from March 1970.

periments, each for a duration of 180 months. The 151 different initial conditions for these forecast experiments were derived from the control experiment. We decided to extend the range of predictions in these experiments as we anticipate that the small errors introduced in these experiments will take longer time to reach saturation. Next, we conducted 151 perturbed forecast experiments. The perturbed forecast experiments were identical to the control forecasts except for a small random perturbation introduced at the initial time on the zonal (U_a) and meridional (V_a) components of the surface winds. The random perturbations had a Gaussian distribution with zero mean and standard deviation of 0.2 ms^{-1} and 0.1 ms^{-1} for perturbations on U_a and V_a respectively. The growth of errors averaged over the 151 cases are shown in Fig. 5. The initial errors in SSTA in this case was identically zero but the small initial errors in the surface winds introduced small errors in the SSTA within one month which grew subsequently. As expected, the smaller initial errors took longer time to reach the saturation value.

Two points are worth noting in Fig. 5. First, the error fluctuates around 1.5°C for the last five years. Thus, we can assume that it has reached its saturation value. Second, we note that the error growth curve has two slopes. This indicates that the growth of errors in the coupled model is

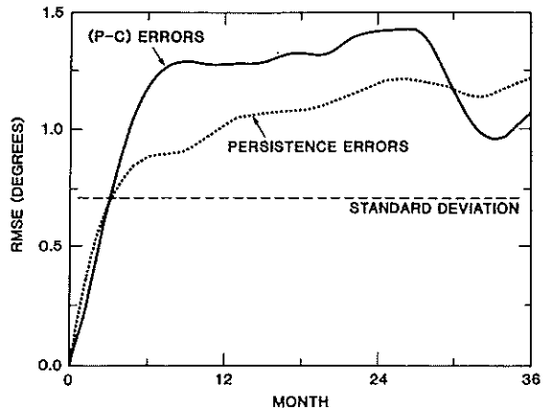

Fig. 3. RMS prediction minus control (P-C) error of NINO3 SSTA using all the 181 predictions. (solid). The persistence error (dotted) and standard deviation (dashed) of the control NINO3 SSTA are also shown.

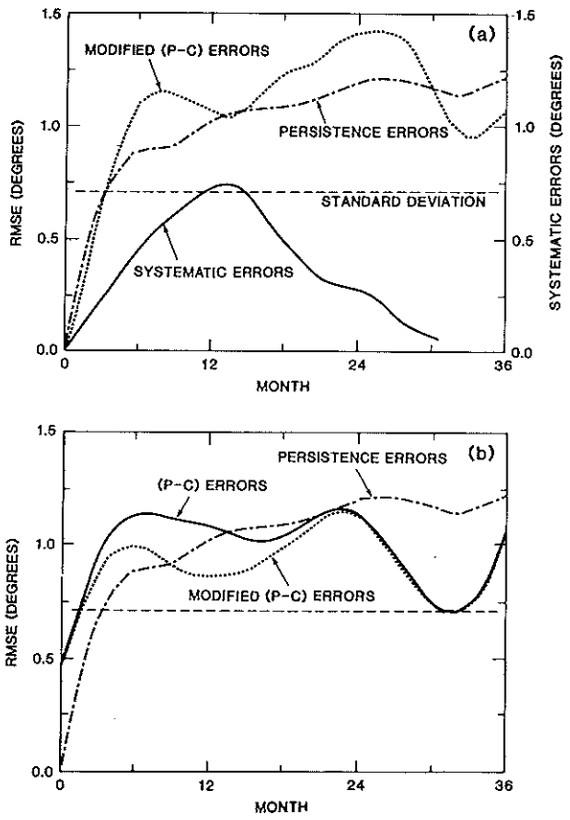

Fig. 4. (a) The systematic error of NINO3 SSTA predictions as defined by mean of all predictions minus mean of all verifications is shown (solid). The modified (P-C) errors (dotted) after removing the systematic error is compared with the persistence (dot-dash) and the standard deviation of the control (dashed). (b) The solid curve is the lagged averaged errors. These predictions are constructed by averaging the six predictions starting from the last six months. The lagged averaged errors after removing the systematic errors (dotted), and the standard deviation (dashed) are also shown.

governed by two processes with two quite different time scales. One of the processes has faster growth rate and tends to saturate at around 1°C and the other has much slower growth rate. In order to obtain some quantitative estimate of the growth rates, we assume that the error growth can be approximated by a linear combination of two processes each governed by a different exponential growth rate. Thus, we write,

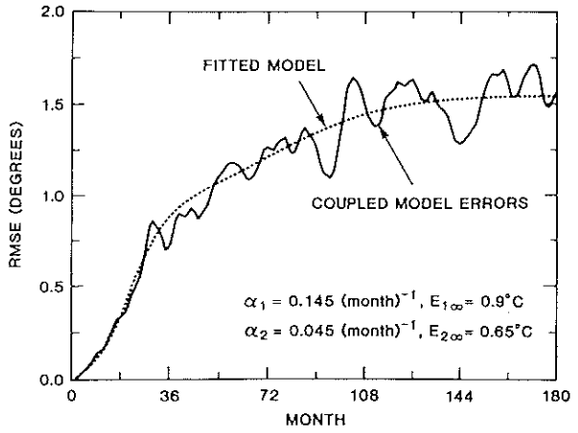

Fig. 5. RMS error from 151 identical twin experiments due to small random initial perturbation on surface winds. The dashed curve is the fitted model.

$$E(t) = E_1(t) + E_2(t), \tag{1}$$

where

$$\frac{dE_1}{dt} = (\alpha_1 E_1 + S_1)(1 - E_1/E_{1\infty}), \tag{2}$$

and

$$\frac{dE_2}{dt} = (\alpha_2 E_2 + S_2)(1 - E_2/E_{2\infty}). \tag{3}$$

As discussed before, α_1 and α_2 represent the two growth rates and the total saturation value is given by $E_\infty = E_{1\infty} + E_{2\infty}$. Similarly, S_1 and S_2 represent two source terms arising due to the inadequacies of the model. We then fitted eqn. (1) to the error growth curve shown in Fig. 5 for which $E_\infty = 1.55$. The best fit is obtained for $E_{1\infty} = 0.9\,^\circ$C. The fast growth rate is found to be $\alpha_1 = 0.145$ (month)$^{-1}$, corresponding to a doubling time of 4.8 months. The slow growth rate is found to be $\alpha_2 = 0.045$ (month)$^{-1}$, corresponding to a doubling time of 15.3 months. The fitted model obtained this way is shown in Fig. 5. The success of the model with two scales acting linearly is rather striking. The existence of two growth rates is also seen in the growth of errors in other variables of the model such as U_a, V_a, NINO4 SSTA, etc.

The existence of a slow scale in the coupled system had been intuitively suggested by Cane and Zebiak (1988) and has been the basis for their optimism for the prediction of the ENSO events at long lead times. These results suggest that indeed there is a basis for optimism for long range predictability of the ENSO events. However, this success will depend on our ability to select those initial conditions that are insensitive to the fast growing instabilities. This may be why forecast made from winter appear to be more predictable. However, a systematic procedure for identifying such initial conditions eludes us at this time.

Mechanisms of aperiodic variability

The finite predictability of the coupled system is a consequence of the aperiodic variability of the system. Understanding the origin of the aperiodic variability of the system is important for understanding the predictability of the coupled system. Therefore, we investigate the factors responsible for the aperiodic variability within the context of the ZC model. Deterministic aperiodicities in most dynamical systems arise due to the intrinsic nonlinearities in the systems. In the ZC model, there are two types of nonlinearities—nonlinearity associated with anomaly temperature advection and nonlinearity associated with the coupling processes. In this part of our study we conducted some sensitivity experiments to examine the sensitivity of the coupled model's variability to the nonlinearities associated with the coupling processes. We show that the nonlinearity associated with the mean seasonal convergence and its feedback on heating of the atmosphere is responsible for the aperiodic or chaotic evolution of the coupled model in the standard case.

In the ZC model, the atmospheric heating is represented by two terms. These two terms are parameterized as,

$$\dot{Q}_s = (\alpha T)\,\exp\left[(\bar{T} - 30\,^\circ\mathrm{C})/16.7\,^\circ\mathrm{C}\right], \tag{4}$$

and

$$\dot{Q}_1^n = \beta\left[M(\bar{c} - c^n) - M(\bar{c})\right], \tag{5}$$

where

$$M(x) = \begin{cases} 0 & x \leqslant 0 \\ x & x > 0 \end{cases} \tag{6}$$

The first term ($\dot{Q}_s$) is a function of the prescribed climatological monthly mean SST and represents the component of the atmospheric heating associ-

ated with the increase in local evaporation due to the increase in the *SST*. We call this part as the heating due to *SST* anomaly (SSTA) feedback. The second term ($\dot{Q}_1''$) represents the component of the atmospheric heating due to increased low level convergence associated with the SSTA induced heating. We call this part as the heating due to convergence feedback. $\bar{c}$ in eqn. (5) is the prescribed climatological monthly mean convergence and c'' is the anomaly convergence induced by the *SST* anomalies in the n^{th} iteration. This part in ZC model is calculated iteratively with a limit $I_{\max}$ on the maximum number of iterations. α and β represent the strengths of the coupling processes corresponding to SSTA feedback and convergence feedback respectively. In the standard version of the ZC model, the dimensional values of α and β are 0.031 $m^2\ s^{-3}/°C$ and $1.6 \times 10^4\ m^2\ s^{-2}$ respectively and $I_{\max}$ is 2. The corresponding nondimensional values of α and β are 1.6 and 0.75 respectively. Since the anomaly convergence is essentially produced by the *SST* anomalies, the locations of c'' is closely related to the location of the *SST* anomalies. However, if this location happens to be a location of climatological mean divergence, it does not produce any heating. In this manner, the feedback is nonlinearly dependent on the climatological mean convergences. The limit on the maximum number of iterations ($I_{\max}$) is set by the authors based on their experimentation with this limit. We found that increase in the number of iterations from 2 does not result in any distinguishable change in the results. In this section, first we present results from a standard run and then examine the sensitivity of the model's variability to changes in the two coupling processes.

In all the time series presentations below, we show area averaged SSTA over NINO3 (5°N–5°S, 90°W–150°W, the solid curve) and NINO4 (5°N–5°S, 160°E–150°W, the dash curve).

In order to have a frame of reference for the model's natural variability, we carried out a long integration (480 years) of the coupled model with standard values of the parameters ($\alpha = 1.6$, $\beta = 0.75$ and $I_{\max} = 2$). The time evolution of the area averaged SSTA over NINO3 and NINO4 for the first 120 years is shown in Fig. 6. Highly aperiodic behavior of the evolution is evident from this figure. There are a few striking features in the variability of the model. Firstly, often there are long periods of inactivity, Such as between 4 and 20 years, between 40 and 60 years. The other thing that is striking is a favored periodicity of about 4 years. Moreover, there is an asymmetry between the matured warm and cold events. Other details of the variability of the model's evolution are discussed at length by Zebiak and Cane (1987, 1988).

Next, we conducted an experiment with the coupled model with the standard strength of the SSTA feedback ($\alpha = 1.6$) but eliminating the convergence feedback by setting $\beta = 0$. This can also be done by setting $I_{\max} = 0$. The evolution of the same area averaged quantities are shown in Fig. 6 (lower panel) for 120 years. It is clear that the absence of the convergence feedback makes the model periodic after a short initial period of adjustment. The periodicity is nearly 4 years. Integrations with a number of other initial conditions show that without the convergence feedback the model always settles down to a similar periodic state. The initial adjustment period ranges from 5 to 10 years for different initial conditions. Thus, it is clear that the fundamental periodicity of about 4 years is a result of equatorial ocean dynamics and SSTA feedback to the atmosphere. However, the aperiodic behavior of the model results mainly from the nonlinearities associated with the convergence feedback.

In order to understand how the transition from periodic to aperiodic behavior of the model takes place as the convergence feedback is introduced, we carried out a series of integrations with increasing strength of the convergence feedback (i.e., by increasing the value of β). We find that the evolution of the model with convergence feedback as strong as or stronger than the standard case is clearly aperiodic. In order to describe the transition to aperiodic behavior more quantitatively, we examined the power spectrum of the NINO3 SSTA time series corresponding to a number of increasing values of β. The spectra of NINO3 SSTA for β corresponding 0.0, 0.5, 0.75 and 1.0 are shown in Fig. 7. As expected, in the absence of the convergence feedback ($\beta = 0$), there is only one

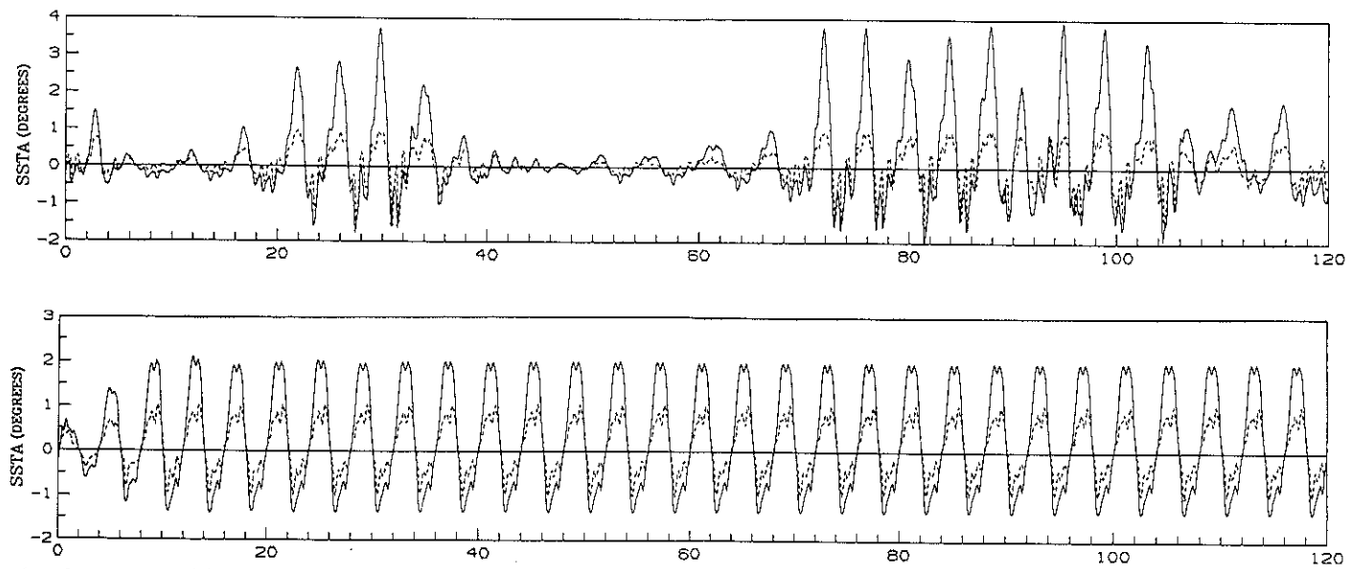

Fig. 6. Time series of area averaged SSTA from the standard run for 120 years with convergence feedback ($\alpha = 1.6$, $\beta = 0.75$ and $I_{max} = 2$). The solid curve is for NINO3 (5°–5°S, 90°–150°W) and the dashed curve is for NINO4 (5°N–5°S, 150°W–160°E). (Upper panel). Time series for the same area averaged SSTA for 120 years without the convergence feedback ($\beta = 0$). (Lower panel)

dominant frequency with period between 48 and 49 months. Two minor periodicities with periods of 24 and 16 months are also seen. It is interesting to note that the fundamental frequency with period of about 48 months remains the dominant frequency even at very high value of β. However, as the strength of convergence feedback is increased, a line broadening takes place around the fundamental frequency. For example, in the standard case ($\beta = 0.75$), almost all periods between 40 months and 75 months are found to have a significant amplitude. For higher values of β, even more periods are excited around the fundamental frequency of 48 months.

We also examined the model's sensitivity with respect to the SSTA feedback in the absence of the convergence feedback. We found that there exists a small window in the strength of the SSTA feedback ($\alpha \approx 1.8$), where the model has aperiodic behavior in the absence of convergence feedback ($\beta = 0$). For higher strength of the SSTA feedback the model again has periodic behavior.

We have seen that the convergence feedback adds a component to the low frequency forcing due to the SSTA feedback that is able to take the low frequency variability from a periodic regime to a nonperiodic regime in the phase space. In order to understand how the convergence feedback forcing operates, we looked at the difference between two runs, one with convergence feedback and the other without it—during very early phases of their evolution. We carried out two sets of 10-day integrations (one time step in the ZC model) one with convergence feedback and one without, for all the 181 initial conditions corresponding to January 1970 through January 1985.

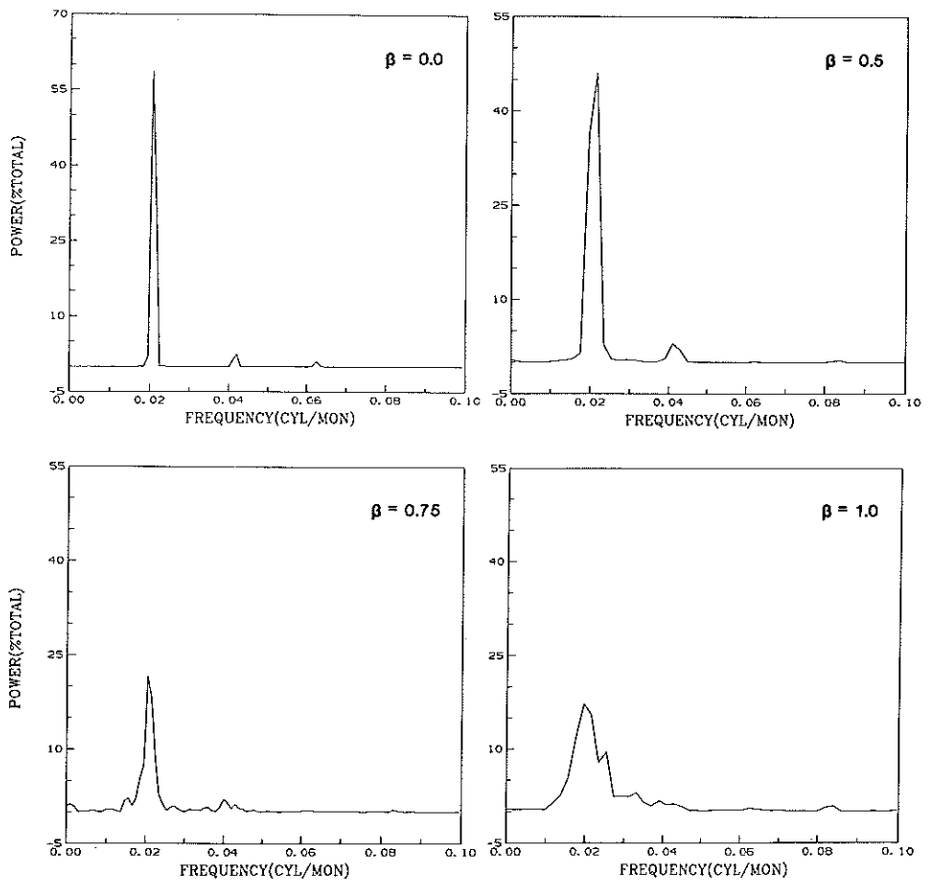

Fig. 7. Power spectrum of NINO3 SSTA from four simulations with four different values of the strength of the convergence feedback (β). Power is shown as percentage of the total power and unit for frequency is cycles per month.

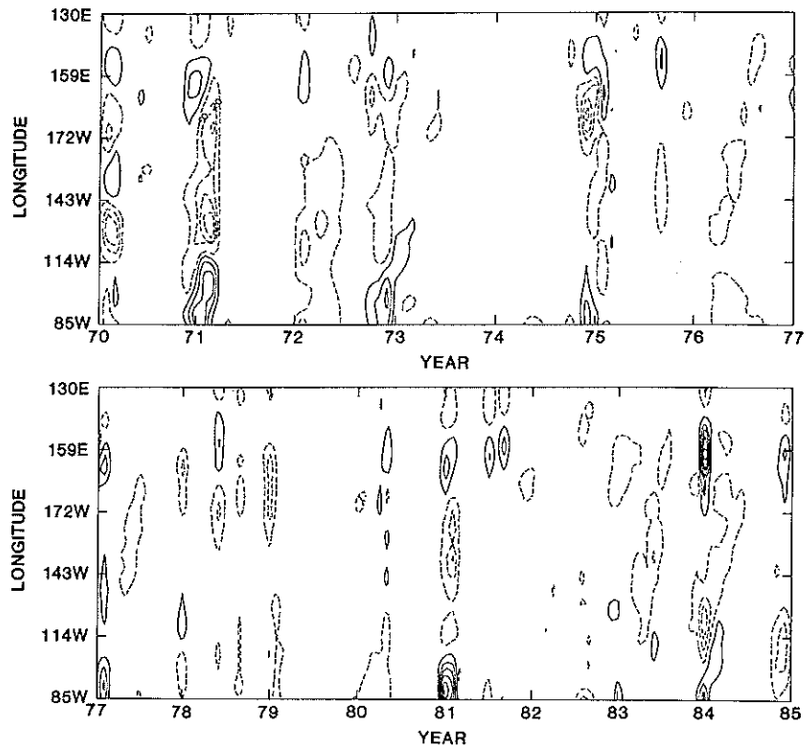

Fig. 8. Time–longitude section of the divergence anomaly difference between two 10-day coupled model simulations, one with and the other without the convergence feedback, averaged over 5°N to 5°S latitude belt. Contour interval is 0.15 and the unit is in 1×10^{-6} s^{-1}. The negative contours are dashed lines. The first negative contour is -0.05 and the first positive contour is 0.1.

Then we calculated the differences (with feedback minus without feedback) between the two runs in different fields. The differences in the anomaly divergence field is illustrative. Figure 8 shows the differences in divergence anomalies between such pairs of runs averaged between 5°N to 5°S for all longitudes and for all the initial conditions. The negative contours represent larger convergence in the case of convergence feedback while positive contours represent larger convergence in the no feedback case.

Thus, the heating associated with the convergence feedback has a tendency to be phase locked with the annual cycle. However, due to the shift of the heating from the early part of the calendar to the middle part of the calendar year during some years other frequencies close to the annual cycle are also introduced. From eqn. (5), we note that the largest response to the convergence feedback would take place if positive SSTA occurs in the region of mean convergence. The largest positive SSTA occurs over the central and eastern equatorial Pacific. Also, the mean convergence field has a clear annual cycle in the eastern part of the Pacific. In particular, the mean field is convergent in this region only during the early part of the calendar year. We believe, this is primarily why the heating associated with the convergence feedback tends to be locked with the annual cycle. However, further investigation is necessary to understand why during some years this response occurs during the early part of the calendar year while during some other years it tends to be shifted to late spring or early summer.

Summary and conclusions

To summarize, a large ensemble of prediction experiments were conducted and a detailed analysis of growth of initial error and forecast errors was carried out. We have compared the *SST* fore-

casts with observations (not shown) as well as the control run. Compared to the control, it is found that the root mean square difference between control and forecasts became larger than the standard deviation of the control as well as persistence error in about three months. However, compared to observations, the errors in the initial condition as given by the control run are comparable to the standard deviation of the observations. We have also noted some significant systematic errors in the model. There is indication that the forecasts may be improved to some extent by averaging a few of the most recent available forecasts and removing the known systematic error.

We also carried out a large ensemble of identical twin experiments, each for a duration of 15 years. In one of each pair of experiments a small random perturbation was introduced at the initial time in the surface winds. These experiments have shown that the growth of small initial errors in the coupled model is governed by process with two well separated time scales. The fast time scale process introduces errors that has doubling time of about 5 months while the slow time scale process introduces errors that has typical doubling time of about 15 months. The existence of such a slow time scale, gives us a basis for optimism in long range forecast of ENSO type events. However, the fast growth rate tends to saturate at a level which is comparable to the climatological standard deviation. Thus, the key to the long range forecasting of the ENSO type events may lie in our ability to identify those initial conditions that are not too sensitive to the processes associated with fast growth rate. We also carried out some diagnostic studies to determine the factors that may be responsible for the growth of prediction errors in the coupled model. We have indicated areas where future improvements in the coupled model may be made.

Within the context of the ZC model, we also investigated the possible mechanisms responsible for the aperiodic behavior of a coupled system. For the set of standard parameters used in the model, we found that the nonlinearity associated with the convergence feedback may be responsible for the aperiodic behavior of the model. In the absence of the convergence feedback, the feedback associated with the air–sea interaction parameterized in terms of the sea surface temperature anomaly (SSTA feedback) results in a periodic oscillation with a periodicity of about 4 years. As the strength of the convergence feedback is increased, the model variability goes from a periodic regime to an aperiodic regime through a broadening of the frequency spectrum around the basic periodicity of about 4 years. This indicates that the coupling associated with the convergence feedback may be looked as a forcing with a finite band frequency spectrum. Examination of the forcing associated with the convergence feedback shows that it has a dominant annual component with relatively large amplitude only during 2 or 3 months of the year. For most of the years studied, the convergence feedback is effective only during the first two or three months of the calendar year. For some other years, it is effective during late spring and early summer. This selected efficiency of the convergence feedback is related to the strong seasonality of the background mean convergence over the eastern Pacific.

Assuming that the basic periodicity of about 4 years in the coupled model may be represented by a delayed oscillator analog model, we found (not shown here) that the basic character of the aperiodic variability in the Zebiak and Cane (1987) model with a broad band frequency spectrum, may be reproduced if the delayed oscillator model is forced by a forcing with a finite band annual cycle.

Acknowledgements

The authors thank Drs. Mark Cane and Steve Zebiak for kindly supplying them with the code of the model and the necessary data to run it. We also benefited greatly from several discussions with Dr. V. Krishnamurthy. We would like to thank Ms. Marlene Schlichtig for typing the manuscript and Ms. Laura Rumberg for drafting the figures.

References

Barnett, T.P., 1983. Interactions of the monsoon and the Pacific trade wind system at interannual time scales. Part I: The equatorial zone. Mon. Weather Rev., 111: 756–773.

Battisti, D.S., 1988. Dynamics and thermodynamics of a warm event in a coupled tropical atmosphere–ocean model. J. Atmos. Sci., 45, 2889–2919.

Cane, M.A. and Zebiak, S.E., 1987. Prediction of El Niño events using a coupled model. In: H. Cattle (Editor), Atmospheric and Oceanic Variability. R. Meteorol. Soc., U.K., 153–181.

Cane, M.A., Zebiak, S.E. and Dolan, S.C., 1986. Experimental forecasts of El Niño. Nature, 321: 827–832.

Goldenberg, S.O. and O'Brien, J.J., 1981. Time and space variability of tropical Pacific wind stress. Mon. Weather Rev., 109, 1190–1207.

Goswami, B.N. and Shukla, J., 1990a. Predictability of a coupled ocean atmosphere model. To appear in J. Climate.

Goswami, B.N. and Shukla, J., 1990b. On a mechanism for the aperiodic variability in a coupled ocean-atmospheric model. Submitted to J. Climate.

Lorenz, E.N., 1982. Atmospheric predictability experiments with a large numerical model. Tellus, 34: 505–513.

Zebiak, S.E. and Cane, M.A., 1987. A model El Niño–Southern Oscillation. Mon. Weather Rev., 115: 2262–2273.

Zebiak, S.E. and M.A. Cane, 1988. Diagnostic studies of a coupled model's climate variability. Proc. 19th Clim. Diagn. Workshop. Atmos. Environ. Res. Inc., Cambridge, Mass. Oct. 31–Nov. 4, 1988. U.S. Dep. Commerce, pp. 283–288.